

Improving selectivity preserving affinity: New piperidine-4-carboxamide derivatives as effective σ_1 -ligands

Daniele Zampieri^{a,*,1}, Erik Laurini^{b,1}, Luciano Vio^a, Maurizio Fermeglia^b,
Sabrina Pricl^{b,c,**}, Bernhard Wünsch^d, Dirk Schepmann^d, Maria Grazia Mamolo^a

^a Department of Chemistry & Pharmaceutical Sciences, Piazzale Europa 1, University of Trieste, 34127 Trieste, Italy

^b Molecular Simulation Engineering (MOSE) Laboratory, DI3, Piazzale Europa 1, University of Trieste, 34127 Trieste, Italy

^c National Interuniversity Consortium for Material Science and Technology (INSTM), Research Unit MOSE-DEA, University of Trieste, Trieste, Italy

^d Department of Pharmaceutical and Medicinal Chemistry, Corrensstrasse 48, 48149 Münster, Germany

ARTICLE INFO

Accepted 11 December 2014

Keywords:

σ -Receptors

Piperidine-4-carboxamide derivatives

Radioligand binding assays

ABSTRACT

We report the design, synthesis and binding evaluation against σ_1 and σ_2 receptors of a series of new piperidine-4-carboxamide derivatives variously substituted on the amide nitrogen atom. Specifically, we assessed the effects exerted on σ receptor affinity by substituting the N-benzylcarboxamide group present on a series of compounds previously synthesized in our laboratory with different cyclic or linear moieties. The synthesized compounds **2a–o** were tested to estimate their affinity and selectivity toward σ_1 and σ_2 receptors. Very high σ_1 affinity ($K_i = 3.7$ nM) and $K_i\sigma_2/K_i\sigma_1$ selectivity ratio (351) were found for the tetrahydroquinoline derivative **2k**, featuring a 4-chlorobenzyl moiety linked to the piperidine nitrogen atom.

1. Introduction

After the initial, erroneous classification as opioid receptor subtype [1], σ receptors (σ -Rs) have been shown to represent a non-opioid, non-phencyclidine but haloperidol-sensitive receptor family [2]. At least two distinct σ receptor subtypes – designated as σ_1 -R and σ_2 -R, respectively – have been identified so far [3–5], characterized by different tissue distribution and dissimilar binding profile [6].

The σ_1 -R, originally cloned from guinea pig liver [7] and then from several other sources including human placenta choriocarcinoma cells [8], consists of 223 amino acids and shares about 90% identity and 95% similarity across species [7]. σ_1 receptors are involved in the regulation of ion channels and in the modulation of neurotransmitter systems [9–11]. Much less is known about the σ_2 receptor subtype. The protein has not been cloned yet, but its molecular weight has been determined as approximately 21.5 kDa

[7] recognized in recent year as a small-ligand operated chaperone essential for the regulation of the passage of Ca^{2+} from the endoplasmic reticulum (ER) to the mitochondria [12a–c]. Recently, its association with the PGRMC-1 (Progesterone Receptor Membrane Component 1) protein has been hypothesized, with subsequent role in signaling and apoptosis [13]. Furthermore, it has been proposed that both σ -R subtypes are involved in cellular apoptotic response [14,15] and in the release of Ca^{2+} via an IP_3 -independent mechanism [16,17].

Many studies described the cytotoxic effects of several σ_1 antagonists and σ_2 agonists [18,19]. However, their impact on cell cycle or mechanisms of cell death is not clearly understood. Further, several synthetic molecules belonging to different structural classes were found to bind to the σ_1 receptor. Among these, (+)-pentazocine, showing high σ_1 -affinity and selectivity, represents a suitable tool for structural and functional studies on σ_1 -R and, as such, is currently used as preferred radioligand [20]. On the other hand, endogenous compounds such as progesterone, D-erythro-sphingosine, and N,N-dimethyltryptamine have good σ_1 -R affinity/selectivity and play an important role in modulating σ_1 -Rs [7,21].

From the medicinal chemistry point of view the design and the development of new, potent and selective σ_1 -R ligands able to interfere with the biological activity of this receptor are becoming crucial issues. Under this perspective, new different structures

* Corresponding author.

** Corresponding author. Molecular Simulation Engineering (MOSE) Laboratory, DI3, Piazzale Europa 1, University of Trieste, 34127 Trieste, Italy.

E-mail addresses: dzampieri@units.it (D. Zampieri), sabrina.pricl@di3.units.it (S. Pricl).

¹ These authors contributed equally to this work.

endowed with σ_1 -R affinity and selectivity, such as benzooxazolones [22a,b], alkyl and arylcarboxamide [22b,23–25], arylalkylamines [26a–f], and spirocyclic pyranopyrazoles [27] were identified and reported by various research groups. In addition, some arylacetamides derivatives synthesized by Huang Y. and coll. [28a,b] showed a remarkable affinity towards σ_1 -R and good selectivity against σ_2 -R subtype. In our previous work we reported the synthesis of some carboxamide derivatives, in which the amide group at position 4 of the piperidine is inverted with respect to the compounds in Huang's series. All our derivatives are endowed with good σ_1 affinity but showing only moderate selectivity towards the σ_2 receptor [22b]. Within this series, compounds **1a,b** (Fig. 1) showed the most interesting σ_1 binding profile ($K_i\sigma_1 = 22.5$ nM and 12.9 nM, respectively) coupled with modest selectivity against the σ_2 subtype ($K_i\sigma_2/K_i\sigma_1 = 8$ and 11, respectively).

As such, both derivatives were exploited to validate a three-dimensional (3D) pharmacophore model [22b] and the only 3D homology model of σ_1 receptor available to date [23]. Importantly, the results of the 3D pharmacophoric modeling offered a molecular-based rationale for the remarkable binding profile of **1b**. As we see from Fig. 2, the structure of this carboxamide derivative is provided with all pharmacophoric requirements for optimal σ_1 binding: the basic piperidine nitrogen atom matches the positive ionizable feature, the amide oxygen atom is able to accept a hydrogen bond from a donor residue on the receptor while the two benzyl rings fulfill the hydrophobic features of the model. Accordingly, the predicted $K_i\sigma_1$ value of 5.5 nM substantiates compound **1b** as a potent σ_1 ligand, in agreement with the experimental $K_i\sigma_1$ affinity of 12.9 nM [22b]. Despite compound **1a** is missing one hydrophobic pharmacophoric feature because of its unsubstituted phenyl ring, its mapping onto the σ_1 -R 3D pharmacophore model (data not shown) confirmed it as a good σ_1 -R binder with a predicted affinity of 37 nM, fairly close to the experimental value (22.5 nM) [22b]. Ultimately, these evidences support the hypothesis that appropriated substitutions on the phenyl ring of these derivatives act as optimizing elements for σ_1 -R ligand binding affinity.

On the basis of the results summarized above, with the aim of improving **1b** σ_1 -R selectivity without affecting its high affinity for this receptor, in the present effort we designed, synthesized and evaluated the binding constants for the new series of piperidine carboxamide derivatives **2a–o** shown in Scheme 1.

As shown in Scheme 1, the N-benzylcarboxamide moiety in **1b** was replaced with various aliphatic or alicyclic moieties (**2a–i**) or with the tetrahydroquinoline and tetrahydroisoquinoline residues (**2j–o**), respectively. Compounds **2a–o** resulted from the application of a computational procedure combining pharmacophore modeling and receptor-based ligand design.

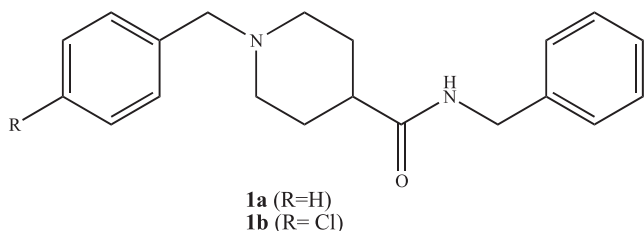


Fig. 1. Structure of lead compounds **1a,b**.

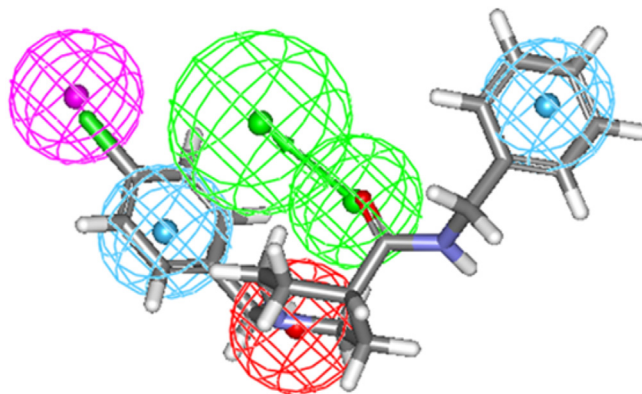


Fig. 2. Mapping of **1b** on the σ_1 receptor 3D pharmacophore model. The hypothesis features are portrayed as meshed spheres, color-coded as follows: red, positive ionizable (PI); light blue, hydrophobic aromatic (HYAR); pink, generic hydrophobic (HY), light green, hydrogen bond acceptor (HBA). (For interpretation of the references to colour in this figure legend, the reader is referred to the web version of this article.)

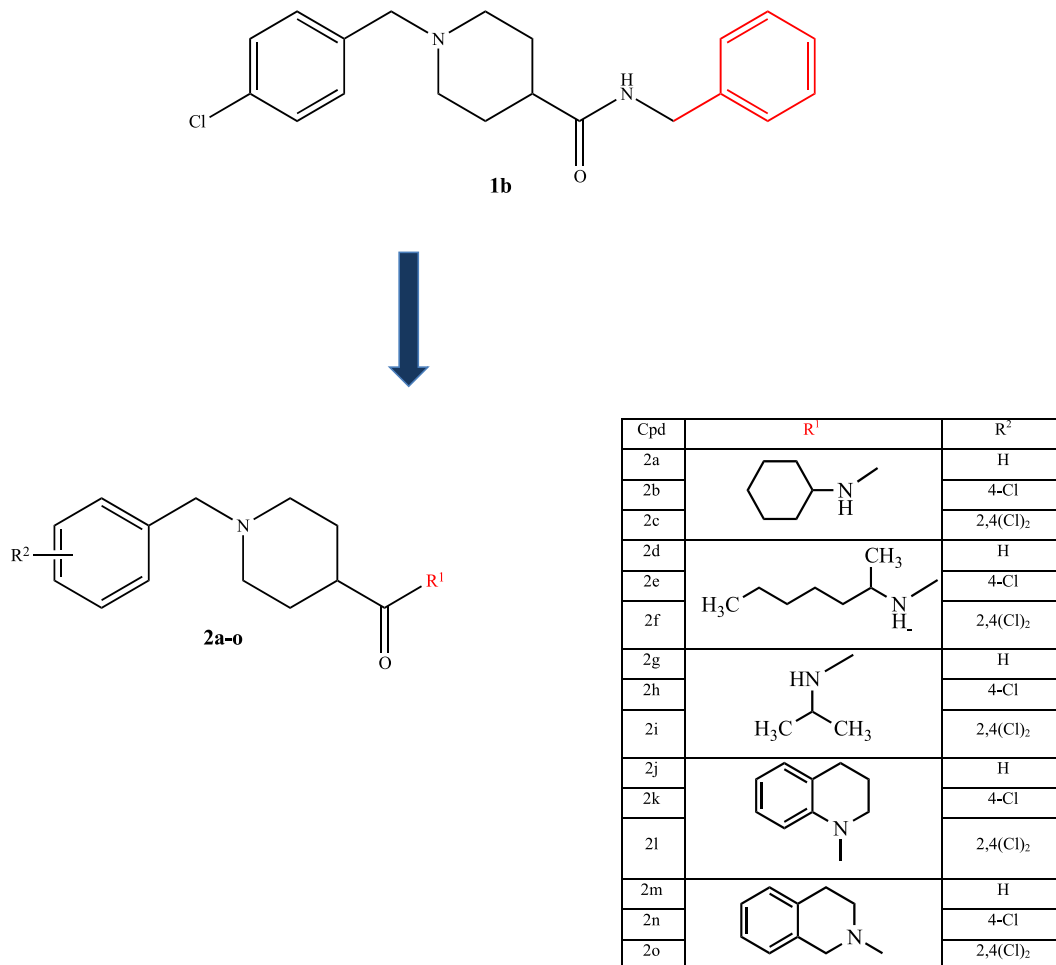
2. Results and discussion

2.1. Molecular modeling

To further rationalize the σ_1 -R affinity of compound **1b** we adopted an *in silico* approach based on the combination of ligand-based (3D-pharmacophore modeling) and receptor-based computational methodologies [22b,23,24] starting from the mapping of the optimized model of **1b** onto our 3D-pharmacophore model (Fig. 2). To get further insight on the molecular interactions between compound **1b** and its biological target we then docked [22–25,27] the optimized structure of **1b** in the putative binding pocket of the 3D σ_1 receptor homology model [22,23] and estimated the corresponding drug/protein free energy of binding (ΔG_{bind}) via MM/PBSA (Molecular Mechanics/Poisson-Boltzmann Surface Area) calculations [29]. As exemplified in Fig. 3, all functional groups identified by pharmacophore mapping establish stabilizing interactions with the σ_1 receptor, confirming the idea that the N-(*p*-chlorobenzyl)piperidine carboxamide (NpCPC) moiety possesses the three prototypical binding requirements characterizing potent σ_1 binders [22–24].

Indeed, the equilibrated MD trajectory of the σ_1 -R/**1b** complex reveals the presence of stabilizing π interactions between the *p*-chlorobenzyl ring of **1b** and the side chains of Trp121 and Arg119. Moreover, the basic nitrogen is engaged in a persistent salt bridge with the COO[−] group of Asp126 while a stable hydrogen bond between the donor hydroxyl group of Thr151 and the acceptor counterpart in the amide moiety of compound **1b** is also detected during the entire course of the MD simulation. Of note, the hydrophobic pocket lined by the side chains of the receptor residues Ile128, Phe133, and Tyr173 with the further stabilizing contribution of Glu172 perfectly encase the unsubstituted phenyl ring of **1b**. As consequence of this favorable binding mode, MM/PBSA endows compounds **1b** with a very good affinity towards the σ_1 receptor, as testified by the calculated binding free energy value of -11.12 kcal/mol (Table 1). As is often the case in protein/ligand binding, the main favorable contribution to ΔG_{bind} is provided by the van der Waals (ΔE_{VDW}) and electrostatic (ΔE_{ELE}) components in the gas phase, while polar solvation energies (ΔG_{PB}) and entropy components ($-T\Delta S$) tend to oppose binding (Table 1).

The driving force leading to σ_1 -R/**1b** complex formation was further investigated by deconvoluting the free energy of binding on a per-residue basis to generate the receptor/residue interaction spectrum presented in Fig. 4.



Scheme 1. Structure of compounds **2a–o**.

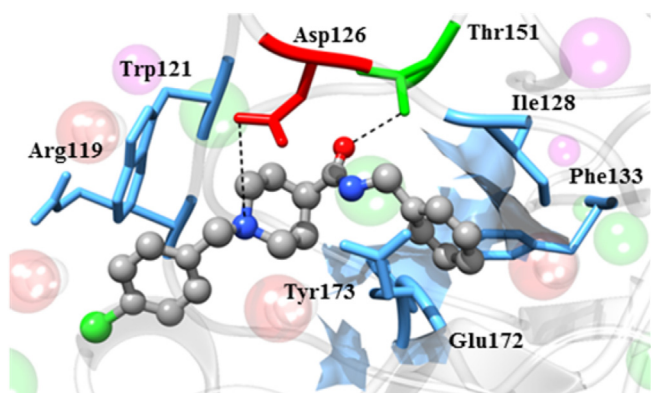


Fig. 3. Equilibrated MD snapshot of the σ_1 receptor in complex with **1b**. The image is a zoomed view of the receptor binding site. The ligand is portrayed in sticks-and-balls and colored by element, while the protein residues mainly involved in the interaction with **1b** are highlighted as colored sticks and labeled. Salt bridges and H-bonds interactions are shown as dotted black lines. Some water molecules and ions are shown as transparent spheres colored by element.

As shown in Fig. 4, all ligand/receptor favorable interactions discussed above are energetically confirmed and quantified by this analysis: the major stabilizing contributions are indeed afforded by the σ_1 -R residues clustering in the region Arg119 – Phe133, besides those yielded by a few other receptor residues such as Thr151,

Glu172, and Tyr173. In detail, the salt bridge between the piperidine $-\text{NH}^+$ atom and the side chain of Asp126 is responsible for a favorable contribution to binding of -2.57 kcal/mol while the hydrogen bond involving the hydroxyl group of Thr151 supports the binding with an enthalpic contribution of -1.85 kcal/mol. Moreover, the encasement of the aromatic 4-chlorophenyl ring by the side chains of the σ_1 receptor residues Arg119, Tyr120 and Trp121 contributes -2.90 kcal/mol of stabilizing van der Waals and hydrophobic interactions. Finally, the insertion of the benzylcarboxamide ring into the binding cavity surrounding the σ_1 -R residue Ile128, Phe133, Glu172, and Tyr173 provides further, overall favorable contribution of -5.89 kcal/mol.

On the basis of these results we proceeded with the design of new carboxamide derivatives able to maintain very good σ_1 -R affinity. To the purpose, we considered that the N-(*p*-chlorobenzyl) piperidine carboxamide scaffold and the corresponding interactions (NpCPCi) were crucial molecular determinants for effective σ_1 -R binding. Thus, to preserve the aromatic characteristics of the substituent in the structure of **1b**, we initially chose to modify the substituent on the amide nitrogen with a cycloalkyl group (**2b**), a bulky or small alkyl moiety (**2e** and **2h**, respectively), and a tetrahydroquinoline (**2k**) and tetrahydroisoquinoline ring (**2n**), respectively. In principle, all these new residues should be efficiently encased in the σ_1 receptor binding pocket and thereby establish the appropriate interactions with residues Ile128, Phe133, Glu172, and Tyr173 as observed for compound **1b**.

Table 1

Binding free energy (ΔG_{bind}) and its components for **1b** in complex with the σ_1 receptor. All energy values are in kcal/mol. The experimental and calculated K_i values (nM) are also reported for comparison.

Components	1b
ΔE_{VDW}	-48.33 ± 0.09
ΔE_{ELE}	-150.12 ± 0.13
ΔE_{MM}	-198.45 ± 0.16
ΔG_{PB}	164.98 ± 0.15
ΔG_{NP}	-5.29 ± 0.01
ΔG_{SOL}	159.69 ± 0.16
ΔH_{bind}	-38.76 ± 0.23
$-T\Delta S_{\text{bind}}$	27.64 ± 0.26
ΔG_{bind}	-11.12 ± 0.34
$K_i\sigma_1(\text{exp})^a$	12.9 ± 0.8
$K_i\sigma_1(\text{calc})^a$	7.1

^a The $K_i\sigma_1(\text{calc})$ values were obtained from the corresponding ΔG_{bind} values using the relationship $\Delta G_{\text{bind}} = -RT \ln(1/K_i)$.

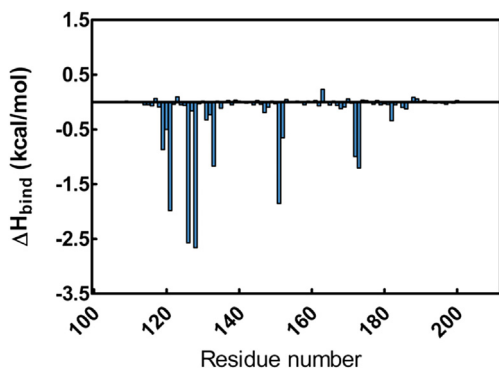


Fig. 4. Per residue binding free energy decomposition for the σ_1 receptor in complex with **1b**. Only σ_1 -R amino acids from position 100 to 200 are shown, as for all the remaining protein residues the contribution to ligand binding is irrelevant.

To validate this hypothesis, before engaging in the synthesis of this new series of σ_1 -R ligands we carried out the same

computational procedure applied to **1b** on the new derivatives and predicted the relevant affinities towards the receptor. These results are listed in **Table 2**.

According to our calculations, all new derivatives exhibited σ_1 receptor affinity values comparable to compound **1b** (**Table 2**) with the notable exception of the N-isopropyl derivative **2h**, for which a strong decrease of the free energy of binding ΔG_{bind} and the $K_i\sigma_1$ were predicted. The best σ_1 binder of the series was the tetrahydroisoquinoline derivative **2n** ($\Delta G_{\text{bind}} = -11.47$ kcal/mol, $K_i\sigma_1(\text{calc})$ of 3.9 nM) for which the optimized conformation assumed in complex within the putative binding pocket of σ_1 receptor is utterly similar to that of its compound precursor **1b**, as illustrated in **Fig. 5A, B** (see SI for details on all other compounds).

Substantially, the tetrahydroisoquinoline substituent allowed preserving the favorable hydrophobic interactions within the receptor binding cavity without affecting the optimal binding pose orientation of the NpCPC portion (**Fig. 5A, B**).

To quantify the effect of the different substituents on the affinity toward the σ_1 receptor, the decomposition of the enthalpic component of ΔG_{bind} was carried out on the entire series of these newly designed compounds. To better rationalize these results, we clustered the contributions of the σ_1 -R residues mainly involved in ligand binding in two subclasses (**Fig. 5C**), defined as follows: i) a contribution afforded by the portion of the molecular structure left unchanged, previously termed NpCPCi and contributed by residues Arg119, Trp121, Asp126, and Thr151, and ii) another contribution brought about by residues Ile128, Phe133, Glu172, and Tyr173 clustered together to represent the global effect of the structure modification on the enthalpy-driven binding.

From **Fig. 5C** we can observe that the replacement of the N-benzyl of compound **1b** with a more rigid aromatic portion (compounds **2k** and **2n**) did not affect both classes of binding interactions while a slight decrease in binding stabilization is detected for the non-aromatic derivatives **2b** and **2e** which, in turn, reflects in a moderate reduction of the corresponding overall receptor affinities ($\Delta G_{\text{bind}} = -10.15$ kcal/mol and $K_i\sigma_1(\text{calc}) = 36$ nM for **2b** and $\Delta G_{\text{bind}} = -9.78$ kcal/mol and $K_i\sigma_1(\text{calc}) = 68$ nM for **2e**, respectively, **Table 2**). Conversely, the N-isopropyl substitution in **2h** led to a strong decrement in favorable binding enthalpy: in fact, the small aliphatic substituent cannot originate the required network of hydrophobic interactions with the side chains of the

Table 2

Binding free energies ΔG_{bind} (kcal/mol) and predicted $K_i\sigma_1(\text{calc})$ values (nM) for **1b**, **2b**, **2e**, **2h**, **2k** and **2n** in complex with the σ_1 receptor. Errors are given in parenthesis as standard errors of the mean. The calculated $K_i\sigma_1(\text{calc})$ (nM) values, as estimated from the corresponding ΔG_{bind} values ($\Delta G_{\text{bind}} = -RT \ln(1/K_i\sigma_1(\text{calc}))$), are also reported.

Compound	R ¹	R ²	ΔH (kcal/mol)	$-T\Delta S$ (kcal/mol)	ΔG_{bind} (kcal/mol)	$K_i\sigma_1(\text{calc})$ [nM]
2b		Cl	-37.47 (0.20)	27.32 (0.28)	-10.15 (0.34)	36
2e		Cl	-37.03 (0.19)	27.25 (0.29)	-9.78 (0.35)	68
2h		Cl	-33.94 (0.23)	26.03 (0.30)	-7.91 (0.38)	1600
2k		Cl	-38.01 (0.21)	27.11 (0.28)	-10.90 (0.35)	10.3
2n		Cl	-38.54 (0.22)	27.07 (0.27)	-11.47 (0.34)	3.9
1b	—	—	-38.76 (0.23)	27.64 (0.26)	-11.12 (0.34)	7.1

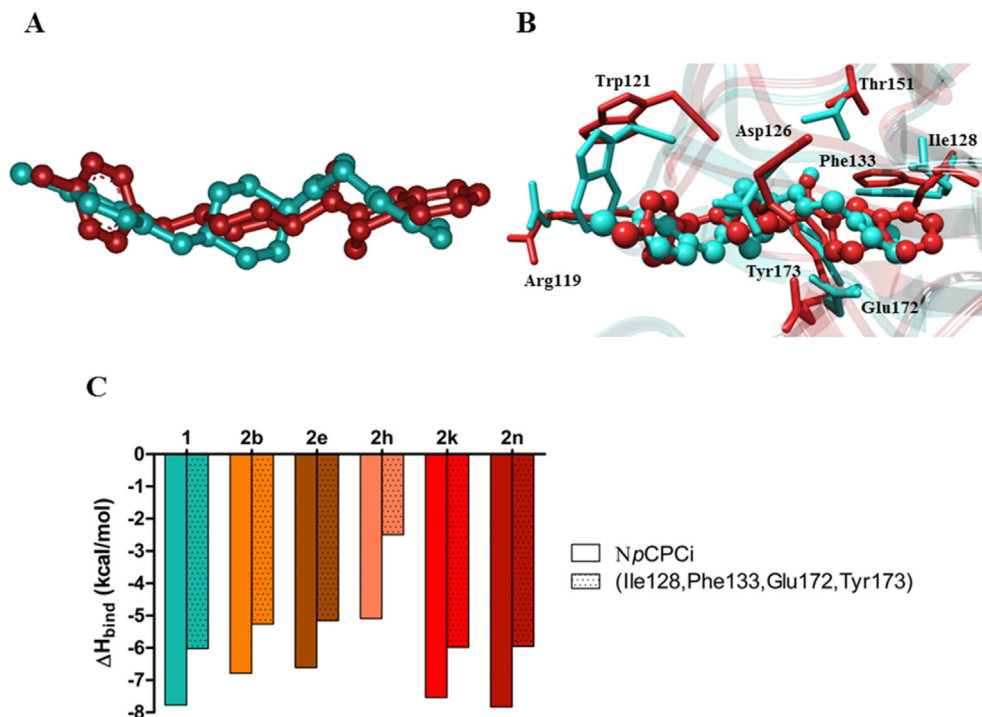


Fig. 5. (A, B) Comparison between the optimized MD binding conformations within the σ_1 receptor putative binding site between compounds **1b** (light see green) and **2n** (firebrick). In both panels, the ligands are portrayed as sticks-and-balls, while the protein residues mainly involved in the interactions with the derivatives are depicted in sticks, labeled and colored accordingly. (C) Comparison of per-residue binding enthalpy decomposition for compounds **1b**, **2b**, **2e**, **2h**, **2k**, and **2n** in complex with the σ_1 receptor. Critical receptor residues are clustered according to the specific underlying interactions as explained in the legend (see also main text for more details). (For interpretation of the references to colour in this figure legend, the reader is referred to the web version of this article.)

residues belonging to the second cluster in Fig. 5C. As a consequence, the ligand assumes an unproductive pose, which exerts a negative influence also on the NpCPCi portion of the receptor binding site (see Figs. S1C and S2C).

The encouraging results predicted by our *in silico* approach discussed above thus prompted us to synthesize the new potential σ_1 -R ligands **2b**, **2e**, **2h**, **2k** and **2n** and test their affinity for the σ_1 receptor in biological assays. Also, based on the previous experimental and *in silico* results achieved with compound **1a** ($\Delta G_{bind} = -10.24$ kcal/mol, $K_i\sigma_1(\text{calc}) = 31$ nM, and $K_i\sigma_1 = 22.5$ nM, [24]), we chose to complete the series of the new carboxamide molecules by synthesizing the corresponding unsubstituted N-benzyl-piperidine derivatives **2a**, **2d**, **2g**, **2j**, and **2m**. Moreover, we further added to the series the 2,4-dichloro derivatives substituted on the same aromatic ring (**2c**, **2f**, **2i**, **2l** and **2o**) since our previous works [22a,b] revealed that this modification decreases the σ_1 -R affinity of the relevant compounds without affecting their σ_2 receptor binding capability. In this way, we could also have a definitive confirmation of the alleged hypothesis according to which the effect on σ_1 -R ligand selectivity in the present series of compounds is borne exclusively by the structural modifications suggested by the computer-based drug-design approach.

3. Chemistry

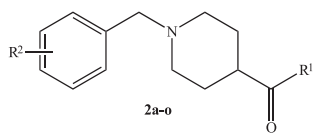
The new piperidine-4-carboxamide derivatives **2a–o** (Table 3) have been prepared (Scheme 2) starting from the commercially available 4-piperidinecarboxylic acid, which was first protected on nitrogen atom with common Boc-anhydride and subsequently treated with SOCl_2 to afford the corresponding acyl chloride. The various amides **3a–e** were obtained *in situ* using the corresponding amines in presence of Et_3N and DMAP and then deprotected with

TFA to afford intermediates **4a–e**. The final step was the N-alkylation of the piperidine nitrogen atom with different benzyl chlorides to produce compounds **2a–o**.

4. Receptor binding studies

The σ_1 and σ_2 receptor affinity of the test compounds was determined in competition experiments by radiometric assays. Compounds **2a–o** were then tested at σ_1 and σ_2 receptors of animal origin prepared from guinea pig brain and rat liver, respectively. The principles of these receptor binding studies are reported in the pharmacology section below; σ_1 -R assays were performed with [^3H]-(+)-pentazocine as radioligand while [^3H]-DTG was used as radioligand in the σ_2 receptor assays.

The collected affinity results for the new derivatives **2a–o** are reported in Table 4. As we can see, all compounds are provided with high σ_1 -R/ σ_2 -R selectivity and some of those exhibited a σ_1 -R affinity very similar to reference compound **1b**, in agreement with the *in silico* predictions. In particular, it was confirmed that the introduction of another chlorine atom in the *ortho* position drastically reduces the σ_1 -R affinity of all 2,4-dichlorosubstituted derivatives (**2c**, **2f**, **2i**, **2l**, and **2o**) while it seems not to affect the affinity for the σ_2 protein. In fact, the $K_i\sigma_1$ values of these molecules are at least one order of magnitude higher compared to those of the corresponding unsubstituted and 4-chloro substituted derivatives. Pleasingly, the introduction of a cyclohexyl moiety (**2a–b**) or a bulky alkyl chain (**2d–e**) on the amide nitrogen atom led to a substantial preservation of the σ_1 -R affinity (7.7–20 nM) paralleled by a strong increment in the selectivity toward the σ_2 -R subtype. Indeed, among the derivative subset **2a–e**, compound **2b** exhibited the best σ_1 receptor affinity ($K_i(\sigma_1) = 7.7$ nM) and highest selectivity ($K_i\sigma_2/K_i\sigma_1 = 234$). On the other hand as predicted by

Table 3
Characterization of derivatives **2a–o**.

Cpd	R ¹	R ²	Yield (%)	M.p. (°C)	CHN
2a		H	26.3	131-3	C ₁₉ H ₂₈ N ₂ O
2b		4-Cl	33.1	165-7	C ₁₉ H ₂₇ ClN ₂ O
2c		2,4(Cl) ₂	24.4	183-5	C ₁₉ H ₂₆ Cl ₂ N ₂ O
2d		H	95.4	Oil	C ₂₀ H ₃₂ N ₂ O
2e		4-Cl	48.4	84-6	C ₂₀ H ₃₁ ClN ₂ O
2f		2,4(Cl) ₂	25.7	89-91	C ₂₀ H ₃₀ Cl ₂ N ₂ O
2g		H	34.9	143-5	C ₁₆ H ₂₄ N ₂ O
2h		4-Cl	43.3	167-9	C ₁₆ H ₂₃ ClN ₂ O
2i		2,4(Cl) ₂	39.8	140-2	C ₁₆ H ₂₂ Cl ₂ N ₂ O
2j		H	62.6	Oil	C ₂₂ H ₂₆ N ₂ O
2k		4-Cl	91.1	Oil	C ₂₂ H ₂₅ ClN ₂ O
2l		2,4(Cl) ₂	91.9	104-7	C ₂₂ H ₂₄ Cl ₂ N ₂ O
2m		H	43.2	82-5	C ₂₂ H ₂₆ N ₂ O
2n		4-Cl	63.6	Oil	C ₂₂ H ₂₅ ClN ₂ O
2o		2,4(Cl) ₂	94.6	Oil	C ₂₂ H ₂₄ Cl ₂ N ₂ O

modeling head of synthesis, compounds **2g–i**, in which the carboxamide nitrogen atom has been linked to a small isopropyl group, are almost devoid of receptor affinity. However, the best result was achieved with the introduction of an aromatic scaffold on the nitrogen atom: 3,4-dihydroquinoline-1(2*H*)-yl derivatives **2j–k** and 3,4-dihydroisoquinoline-2(1*H*)-yl derivatives **2m–n** are, in effect, the most active compounds of the entire series, with $K_i\sigma_1$ values of 4.6, 3.7, 8.8, and 8.0 nM respectively. Importantly, the selectivity of these derivatives is very high, with compound **2j** endowed with the best $K_i\sigma_2/K_i\sigma_1$ ratio (>435).

As a final step we checked the selectivity spectrum of the new

σ_1 -R ligands **2a–o** by testing them against other receptor systems such as NMDA (Table 4). As we can see from the affinity values reported in Table 4, none of the compounds exhibited considerable NMDA affinity, highlighting once again their intrinsic preference towards σ_1 receptors.

5. Conclusions

Compound **1b**, endowed with high σ_1 receptor affinity ($K_i\sigma_1 = 12.9$ nM) has been chosen as lead compound for computational design and subsequent synthesis of a new series of derivatives **2a–o**, with the aim of improving the original low selectivity with respect to the σ_2 receptor subtype. In the design process we maintained the *N*-*p*-chlorobenzylpiperidine-4-carboxamide scaffold of **1b**, whereas the benzyl moiety linked to the amide nitrogen atom has been replaced with cycloalkyl (**2b**) and alkyl (**2e** and **2h**) groups or with residues containing an aromatic ring as the 3,4-dihydroquinolin-1(2*H*)-yl (**2k**) or 3,4-dihydroisoquinolin-2(1*H*)-yl moieties (**2n**). Once synthesized and characterized the new series of potential σ_1 -R binders, we evaluated their biological affinity against σ receptors and NMDA receptor (PCP site).

From the view point of the σ_1 -R ligand molecular structure requirements, the main results of our combined *in silico/in vitro* efforts can be summarized as follows:

(i) with respect to the lead compound **1b**, hydrophobic moieties as bulky alkyl, cycloalkyl or residues containing an aromatic ring linked to the amide nitrogen atom preserved good σ_1 -R affinity and, at the same time, improved selectivity towards the σ_2 receptor; (ii) small alkyl groups (e.g., isopropyl) are not able to generate the necessary hydrophobic interaction within the receptor binding pocket for an optimal binding, so that the corresponding derivatives were almost devoid of σ_1 -R affinity; and (iii) the 2,4-dichloro substitution on the *N*-benzylpiperidine moiety strongly reduced the σ_1 -R affinity.

The data presented in this work constitute an important starting point for the design and synthesis of new σ_1 receptor binders able to establish optimized, stabilizing interactions with both clusters of receptor residues mainly involved in protein/ligand complex formation.

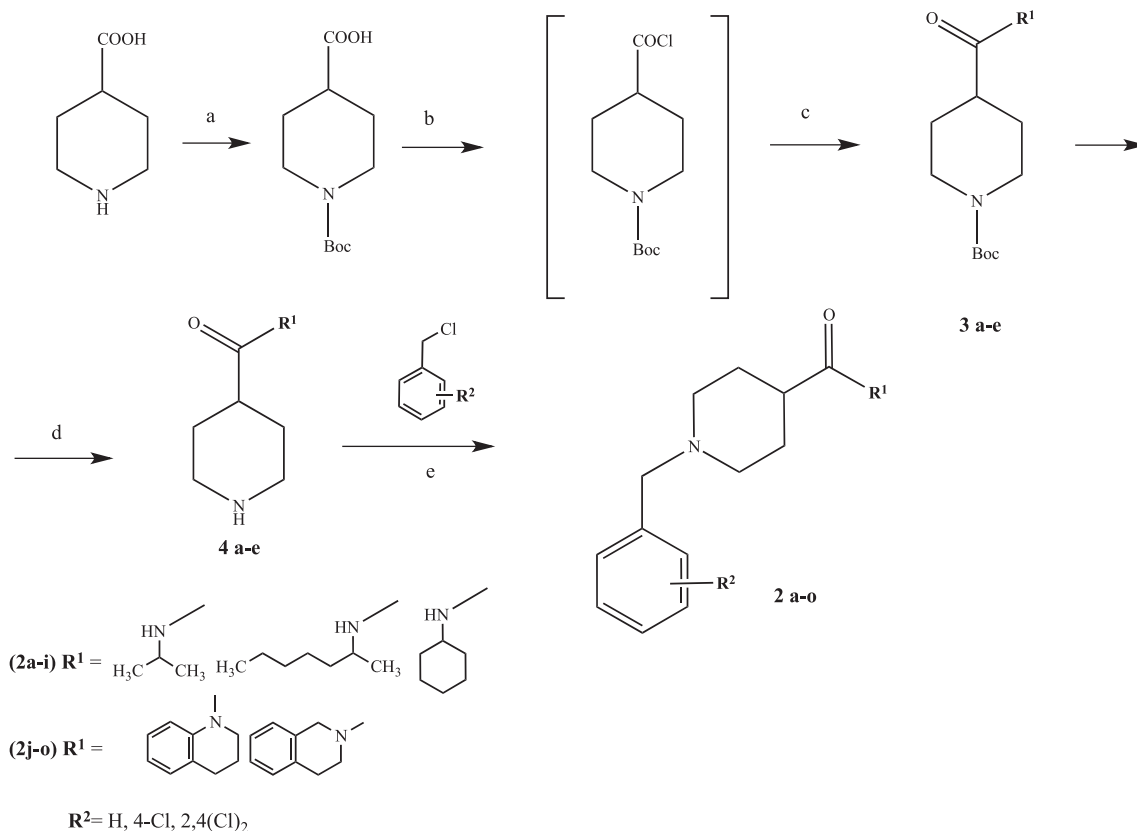
Lastly, due to their specificity the best compounds of this new carboxamide series could be exploited in further, specific biological tests on the σ_1 receptor activity with the purpose of obtaining more information about the pharmacological pathways of this very interesting target.

6. Experimental

6.1. Computational details

The optimized structure of selected compounds **2b**, **2c**, **2h**, **2k** and **2n** was docked into the σ_1 -R putative binding pockets by applying a consolidated procedure [23–26,29]. All docking experiments were performed with *Autodock 4.3/Autodock Tools 1.4.6* [31] on a win64 platform. The resulting docked conformations were clustered and visualized; then, for each compound, only the molecular conformation satisfying the combined criteria of having the lowest (i.e., more favorable) Autodock energy and belonging to a highly populated cluster was selected to carry for further modeling.

The ligand/ σ_1 -R complex obtained from the docking procedure was further refined in *Amber 12* [31] using the quenched molecular dynamics (QMD) method as previously described [23–26,29]. According to QMD, the best energy configuration of each complex resulting from this step was subsequently solvated by a cubic box of TIP3P [33] water molecules extending at least 10 Å in each direction



Scheme 2. Reagents and conditions: a) Boc_2O , K_2CO_3 , THF/ H_2O , 4 h rt; b) SOCl_2/Py ; c) $\text{R-NH-R}'$, Et_3N , DMAP, CH_2Cl_2 , 14 h rt; d) TFA 24 h, rt; e) Acetone, K_2CO_3 , 4 h, reflux.

from the solute. The system was neutralized and the solution ionic strength was adjusted to the physiological value of 0.15 M by adding the required amounts of Na^+ and Cl^- ions. Each solvated system was relaxed by 500 steps of steepest descent followed by 500 other conjugate-gradient minimization steps and then gradually heated to a target temperature of 300 K in intervals of 50 ps of NVT MD, using a Verlet integration time step of 1.0 fs. The Langevin thermostat was used to control temperature, with a collision frequency of 2.0 ps^{-1} . The protein was restrained with a force constant of $2.0 \text{ kcal}/(\text{mol } \text{Å})$, and all simulations were carried out with periodic boundary conditions. Subsequently, the density of the system was equilibrated via MD runs in the isothermal–isobaric (NPT) ensemble, with isotropic position scaling and a pressure relaxation time of 1.0 ps, for 50 ps with a time step of 1 fs. All restraints on the protein atoms were then removed, and each system was further equilibrated using NPT MD runs at 300 K, with a pressure relaxation time of 2.0 ps. Three equilibration steps were performed, each 2 ns long and with a time step of 2.0 fs. To check the system stability, the fluctuations of the rmsd of the simulated position of the backbone atoms of the σ_1 receptor with respect to those of the initial protein were monitored. All chemico-physical parameters and rmsd values showed very low fluctuations at the end of the equilibration process, indicating that the systems reached a true equilibrium condition.

The equilibration phase was followed by a data production run consisting of 40 ns of MD simulations in the canonical (NVT) ensemble. Only the last 20 ns of each equilibrated MD trajectory were considered for statistical data collections. A total of 1000 trajectory snapshots were analyzed the each ligand/receptor complex.

The binding free energy, ΔG_{bind} , between the two ligands and

the σ_1 receptor was estimated by resorting to the MM/PBSA approach implemented in Amber 12. According to this well-validated methodology [23–26,29–34], the free energy was calculated for each molecular species (complex, receptor, and ligand), and the binding free energy was computed as the difference:

$$\Delta G_{\text{bind}} = G_{\text{complex}} - (G_{\text{receptor}} + G_{\text{ligand}}) = \Delta E_{\text{MM}} + \Delta G_{\text{sol}} - T\Delta S$$

in which ΔE_{MM} represents the molecular mechanics energy, ΔG_{sol} includes the solvation free energy and $T\Delta S$ is the conformational entropy upon ligand binding.

The *per residue* binding free energy decomposition was performed exploiting the MD trajectory of each given compound/ σ_1 -R complex, with the aim of identifying the key residues involved in the ligand–receptor interaction. This analysis was carried out using the MM/GBSA approach [35], and was based on the same snapshots used in the binding free energy calculation.

All simulations were carried out using the *Pmemd* modules of Amber 12, running on the EURORA-CPU/GPU calculation cluster of the CINECA supercomputer facility (Bologna, Italy). The entire MD simulation and data analysis procedure was optimized by integrating Amber 12 in modeFRONTIER, a multidisciplinary and multi-objective optimization and design environment [36].

6.2. Chemistry, general methods

Melting points were determined with a Buchi 510 capillary apparatus, and are uncorrected. Infrared spectra in nujol mulls were recorded on a Perkin Elmer Spectrum RXI. Proton nuclear magnetic resonance (^1H NMR) spectra were determined on a

Table 4
Affinities towards σ_1 -R, σ_2 -R and NMDA (PCP site) of the synthesized compounds **2a–o** and haloperidol, DTG, and MK.801 as reference compounds. In case of NMDA the inhibition of the radioligand [3 H]-MK-801 at a concentration of 1 μ M of the respective test compound is given.

Cpd	$K_i \pm \text{SEM (nM)}^a$		σ_2 -R/ σ_1 -R selectivity	NMDA (PCP)
	σ_1	σ_2	$K_i\sigma_2/K_i\sigma_1$	% Inhibition
2a	15.0 \pm 1	>2000	>133	10
2b	7.7 \pm 1.4	1800	234	11
2c	52.0 \pm 16	>2000	>38	20
2d	19.0 \pm 1	>2000	>105	29
2e	20.0 \pm 1	622	31.1	36
2f	125	1200	9.6	17
2g	1070	>2000	>2	33
2h	637	>2000	>3	42
2i	>2000	>2000	n.d. ^b	24
2j	4.6 \pm 1.2	>2000	>435	19
2k	3.7 \pm 0.1	1300	351	34
2l	138	>2000	>14	22
2m	8.8 \pm 0.2	1200	136	42
2n	8.0 \pm 2.9	627	78	37
2o	61.0 \pm 7	662	11	13
1b	12.9 \pm 0.8	146	11	–
Haloperidol	6.6 \pm 0.9	78 \pm 2.0	12	n.d. ^b
DTG	71 \pm 8	54 \pm 8	0.8	n.d. ^b
MK-801	n.d.	n.d.	–	3.4 \pm 0.8

^a Triplicates were performed only for high affinity compounds (<100 nM).

^b Not determined.

Varian Gemini 200 spectrometer, chemical shifts are reported as δ (ppm) in CDCl₃ solution (0.05% v/v TMS). Reaction courses and product mixtures were routinely monitored by thin-layer chromatography (TLC) on silica gel precoated F₂₅₄ Merck plates generally with CHCl₃/EtOH (9:1) as eluent phase. ESI-MS spectra were obtained on a PE-API I spectrometer by infusion of a solution of the sample in MeOH. Elemental analyses (C, H, N) were performed on a Carlo Erba analyzer and were within \pm 0.3 of the theoretical value.

All the commercially available reactants and solvents were purchase from Sigma–Aldrich, Fluka Chemicals and Merk.

6.2.1. General procedure for the preparation of various 1-(tert-butoxycarbonyl)piperidine-4-carboxamide derivatives **3a–e**

To a mixture of N-Boc-4-piperidinecarboxylic acid (3.00 g, 13.1 mmol), pyridine (2.59 g, 32.7 mmol), CH₂Cl₂ (40 mL) and SOCl₂ (1.87 g, 15.7 mmol) were added, under N₂ atmosphere at room temperature, while stirring. After 30 min, a solution of cyclohexylamine (1.43 g, 14.4 mmol), Et₃N (4.24 g, 41.9 mmol), and a catalytic amount of DMAP in CH₂Cl₂ (20 mL) was added dropwise. The reaction was monitored by TLC. After 12 h, the organic phase was washed with 1 N HCl (2 \times 20 mL) and distilled water (2 \times 20 mL), dried with Na₂SO₄, and concentrated in vacuum to give 3.25 g (80%) of tert-butyl 4-(cyclohexylcarbamoyl)piperidine-1-carboxylate **3a** as a light-brown solid; mp 129–133 °C.

¹H NMR (CDCl₃-TMS) ppm (δ): 1.02–2.00 (m, 14H, cyclohex. and pip.); 1.38 (s, 9H, 3(CH₃), Boc); 2.10 (m, 1H, CH, pip., J = 8.05 Hz); 2.66 (t, 2H, CH₂, pip.); 3.68 (m, 1H, CH cyclohex.); 4.06 (m, 2H, CH₂, pip.); 4.23 (broad sign., 1H, (CO)NH, disappearing on deuteration). MS: m/z 311 [MH⁺].

In an analogous way the following compounds **3b–e** were obtained.

6.2.2. tert-Butyl 4-(heptan-2-ylcarbamoyl)piperidine-1-carboxylate **3b**

Oil Yield (%): 72. ¹H NMR (CDCl₃/TMS) δ : 0.85 (t, 3H, CH₃, hept., J = 6.59 Hz); 1.09 (d, 3H, CH₃, hept., J = 6.50 Hz); 1.18–2.20 (m, 12H, hept. and pip.); 1.44 (s, 9H, 3(CH₃), Boc); 2.10–2.50 (m, 1H, CH, pip.); 2.80 (m, 2H, CH₂, pip.); 4.00 (m, 4H, CH hept., CH₂ pip. and NH

disappearing on deuteration). MS: m/z 327 [MH⁺].

6.2.3. tert-Butyl 4-(isopropylcarbamoyl)piperidine-1-carboxylate **3c**

Oil Yield (%): 67. ¹H NMR (CDCl₃/TMS) δ : 1.11 (d, 6H, 2(CH₃) isopr., J = 6.59 Hz); 1.40–2.00 (m, 4H, CH₂, pip.); 1.43 (s, 9H, 3(CH₃), Boc); 2.04–2.55 (m, 1H, CH, pip.); 2.76 (m, 2H, CH₂, pip.); 4.06 (m, 3H, CH isopr., CH₂ pip.) 5.41 (d, 1H, NH disappearing on deuteration, J = 7.32 Hz). MS: m/z 271 [MH⁺].

6.2.4. tert-Butyl 4-(1,2,3,4-tetrahydroquinoline-1-carbonyl)piperidine-1-carboxylate **3d**

Oil Yield (%): 88. ¹H NMR (CDCl₃/TMS) δ : 1.38 (s, 9H, 3(CH₃), Boc); 1.50–1.80 (m, 4H, 2(CH₂), pip. and H_{3,3'} tetrahydroq.); 1.90 (t, 2H, CH₂, pip., J = 6.59 Hz); 2.44–2.70 (t and m, 4H, 2(CH₂), pip. and H_{4,4'} tetrahydroq., J = 6.59 Hz); 2.93 (m, 1H, CH, pip.); 3.72 (m, 2H, CH₂, H_{2,2'} tetrahydroq., J = 6.59 Hz) 4.04 (d, 2H, CH₂, pip.); 7.20 (m, 4H, arom.). MS: m/z 345 [MH⁺].

6.2.5. tert-Butyl 4-(1,2,3,4-tetrahydroisoquinoline-2-carbonyl)piperidine-1-carboxylate **3e**

Oil Yield (%): 92. ¹H NMR (CDCl₃/TMS) δ : 1.38 (s, 9H, 3(CH₃), Boc); 1.65 (m, 4H, CH₂, pip.); 2.60–2.80 (m, 5H, CH and 2(CH₂), pip. and H_{4,4'} tetrahydroisoq.); 3.67 (m, 2H, CH₂, H_{3,3'} tetrahydroisoq., J = 5.86 Hz); 4.10 (d, 2H, CH₂, pip.); 6.64 (d, 2H, H_{1,1'} tetrahydroisoq., J = 10.98 Hz); 7.10 (m, 4H, arom.). MS: m/z 345 [MH⁺].

6.2.6. General procedure for the deprotection of various carboxamide into corresponding derivatives **4a–e**

Trifluoroacetic acid (5 mL) was added to 0.50 g (1.61 mmol) of the compound **4a** and the reaction was stirred, under N₂ atmosphere, overnight. The excess of trifluoroacetic acid was eliminated under reduced pressure and the residue was taken by water and washed with diethyl ether. The aqueous layer was alcalinized to pH 12 (NaOH 10%) and extracted with CH₂Cl₂. The organic phase was then washed with distilled water, dried over anhydrous Na₂SO₄ and filtered. A light-yellow solid of N-cyclohexylpiperidine-4-carboxamide **4a** was obtained (0.21 g; yield (%): 62); mp 163–167 °C.

¹H NMR (CDCl₃-TMS) ppm (δ): 1.02–2.00 (m 14H, cyclohex. and pip., NH pip.); 2.10 (m, 1H, CH, pip.); 2.54 (t, 2H, CH₂, pip.); 3.10 (d, 2H, CH₂, pip.); 3.68 (m, 1H, CH cyclohex.); 4.20 (broad sign., 1H, (CO)NH, disappearing on deuteration). MS: m/z 211 [MH⁺].

In the same way the following compounds **4b–e** were obtained.

6.2.7. N-(heptan-2-yl)piperidine-4-carboxamide **4b**

Oil Yield (%): 46. ¹H NMR (CDCl₃-TMS) ppm (δ): 0.80 (t, 3H, CH₃, hept., J = 6.59 Hz); 1.03 (d, 3H, CH₃, hept., J = 6.59 Hz); 1.13–1.84 (m, 12H, 6(CH₂) hept. and pip.); 2.02–2.26 (m, 1H, CH pip.); 2.18 (broad sign., 1H, NH, pip., disapp. on deuteration); 2.56 (t, 2H, CH₂, pip., J = 12.08 Hz); 3.08 (d, 2H, CH₂, pip., J = 12.08 Hz); 3.91 (m, 1H, CH, hept.); 5.30 (d, 1H, (CO)NH disappearing on deuteration). MS: m/z 227 [MH⁺].

6.2.8. N-isopropylpiperidine-4-carboxamide **4c**

Light-yellow solid; M.p.: 125–127 °C; Yield (%): 60. ¹H NMR (CDCl₃/TMS) ppm (δ): 1.07 (d, 6H, 2(CH₃), isopr., J = 6.59 Hz); 1.13–2.20 (m, 4H, CH₂, pip.); 2.01 (d broad, 1H, NH, disappearing on deuteration); 2.13 (m, 1H, CH, pip.); 2.57 (t, 2H, CH₂, pip., J = 12.45 Hz); 3.08 (d, 2H, CH₂, pip., J = 12.45 Hz); 4.02 (m, 1H, CH isopr.) 5.24 (broad sign., 1H, NH disappearing on deuteration, J = 7.32 Hz). MS: m/z 171 [MH⁺].

6.2.9. (3,4-Dihydroquinolin-1(2H)-yl) (piperidin-4-yl)methanone

4d

Oil Yield (%): 82. ¹H NMR (CDCl₃/TMS) ppm (δ): 1.40–1.80 (m, 5H, 2(CH₂), pip. and H_{3,3'} tetrahydroq., NH); 1.90 (t, 2H, CH₂, pip., *J* = 6.59 Hz); 2.44 (dt, 2H, CH₂, pip.); 2.64 (t, 2H, CH₂, H_{4,4'} tetrahydroq., *J* = 6.59 Hz); 2.80–2.91 (m, 3H, CH and CH₂, pip.); 3.72 (m, 2H, CH₂, H_{2,2'} tetrahydroq., *J* = 6.59 Hz) 7.11 (m, 4H, arom.). MS: *m/z* 245 [MH⁺].

6.2.10. (3,4-Dihydroisoquinolin-2(1H)-yl) (piperidin-4-yl) methanone 4e

Oil Yield (%): 70. ¹H NMR (CDCl₃/TMS) ppm (δ): 1.68 (m, 4H, 2(CH₂), pip.); 2.42 (broad sign., 1H, NH disapp. on deuteration); 2.55–2.90 (m, 5H, CH and 2× CH₂, pip. and H_{4,4'} tetrahydroisoq.); 3.12 (d, 2H, CH₂, pip.); 3.67 (m, 2H, CH₂, H_{3,3'} tetrahydroisoq., *J* = 10.98 Hz); 7.12 (m, 4H, arom.). MS: *m/z* 245 [MH⁺].

6.2.11. Synthesis of the final piperidine-4-carboxamide derivatives 2a–o

Compound **4a** (0.16 g, 0.76 mmol) and K₂CO₃ (0.13 g, 0.91 mmol) was dissolved in 50 mL of acetone and 0.10 g (0.76 mmol) of benzyl chloride was added to the solution. The reaction was allowed to stirring under reflux for 4 h (monitored by TLC) then solvent was eliminated under vacuum and the residue was washed with water then with diethyl ether to afford a white solid of 1-benzyl-N-cyclohexylpiperidine-4-carboxamide **2a**.

Melting point: 131–133 °C. Yield (%): 26. I.R. cm⁻¹ (nujol): 1632, 3221. ¹H NMR (CDCl₃/TMS) ppm (δ): 0.90–2.00 (m, 17H, cyclohex. and pip.); 2.88 (d, 2H, CH₂, pip.); 3.43 (s, 2H, –CH₂–Ph); 3.70 (m, 1H, CH, cyclohex.); 5.26 (broad sign., 1H, NH, disapp. on deuteration); 7.25 (m, 5H, arom.). MS: *m/z* 301 [MH⁺]. Anal. calcd. for C₁₉H₂₈N₂O (MW 300.44): C, 75.96; H, 9.39; N, 9.32%; found: C, 73.80; H, 9.20; N, 9.10%.

In a similar way, starting from compounds **4b–e** and benzyl, 4-chlorobenzyl and 2,4-dichlorobenzyl chloride respectively, derivatives **2b–o** were obtained.

6.2.12. 1-(4-Chlorobenzyl)-N-cyclohexylpiperidine-4-carboxamide 2b

White solid, melting point: 165–167 °C. Yield (%): 33. I.R. cm⁻¹ (nujol): 1627, 3239. ¹H NMR (CDCl₃/TMS) ppm (δ): 0.90–2.00 (m, 17H, cyclohex. and pip.); 2.81 (d, 2H, CH₂, pip.); 3.40 (s, 2H, –CH₂–Ar); 3.70 (m, 1H, CH, cyclohex.); 5.22 (broad sign., 1H, NH, disapp. on deuteration); 7.20 (m, 4H, arom.). MS: *m/z* 335 [MH⁺], 337 [MH⁺+2]. Anal. calcd. for C₁₉H₂₇ClN₂O (MW 334.88): C, 75.96; H, 9.39; N, 9.32%; found: C, 73.80; H, 9.20; N, 9.10%.

6.2.13. 1-(2,4-Dichlorobenzyl)-N-cyclohexylpiperidine-4-carboxamide 2c

White solid, melting point: 183–185 °C. Yield (%): 25. I.R. cm⁻¹ (nujol): 1639, 3280. ¹H NMR (CDCl₃/TMS) ppm (δ): 0.90–2.10 (m, 17H, cyclohex. and pip.); 2.84 (d, 2H, CH₂, pip.); 3.50 (s, 2H, –CH₂–Ar); 3.70 (m, 1H, CH, cyclohex.); 5.22 (broad sign., 1H, NH, disapp. on deuteration); 7.12–7.42 (m, 3H, arom.). MS: *m/z* 369 [MH⁺], 371 [MH⁺+2]. Anal. calcd. for C₁₉H₂₆Cl₂N₂O (MW 369.33): C, 61.79; H, 7.10; N, 7.58%; found: C, 61.60; H, 7.00; N, 7.30%.

6.2.14. 1-Benzyl-N-(heptan-2-yl)piperidine-4-carboxamide 2d

Oil Yield (%): 95. I.R. cm⁻¹ (nujol): 1634, 3269. ¹H NMR (CDCl₃/TMS) ppm (δ): 0.80 (t, 3H, CH₃, hept., *J* = 5.86 Hz); 1.10 (d, 3H, CH₃, hept., *J* = 6.59 Hz); 1.10–2.00 (m, 15H, 7(CH₂), CH hept. and pip.); 2.90 (d, 2H, CH₂, pip.); 3.46 (s, 2H, –CH₂–Ph); 3.90 (m, 1H, CH, hept., *J* = 6.59 and 7.32 Hz); 5.20 (d broad, 1H, (CO)NH disappearing on deuteration, *J* = 7.93 Hz); 7.10–7.30 (m, 5H, arom.). MS: *m/z* 317 [MH⁺]. Anal. calcd. for C₂₀H₃₂N₂O (MW 316.48): C, 75.90; H, 10.19;

N, 8.85%; found: C, 75.80; H, 9.90; N, 8.60%.

6.2.15. 1-(4-Chlorobenzyl)-N-(heptan-2-yl)piperidine-4-carboxamide 2e

White solid, melting point: 84–86 °C. Yield (%): 48. I.R. cm⁻¹ (nujol): 1635, 3251. ¹H NMR (CDCl₃/TMS) ppm (δ): 0.80 (t, 3H, CH₃, hept., *J* = 6.10 Hz); 1.10 (d, 3H, CH₃, hept., *J* = 6.71 Hz); 1.10–2.10 (m, 15H, 7(CH₂), CH hept. and pip.); 2.84 (d, 2H, CH₂, pip.); 3.39 (s, 2H, –CH₂–Ar); 3.92 (m, 1H, CH, hept., *J* = 6.71 and 7.93 Hz); 5.20 (d broad, 1H, (CO)NH disappearing on deuteration, *J* = 7.93 Hz); 7.20 (m, 4H, arom.). MS: *m/z* 351 [MH⁺], 353 [MH⁺+2]. Anal. calcd. for C₂₀H₃₁ClN₂O (MW 350.93): C, 68.45; H, 8.90; N, 7.98%; found: C, 68.50; H, 8.90; N, 8.20%.

6.2.16. 1-(2,4-Dichlorobenzyl)-N-(heptan-2-yl)piperidine-4-carboxamide 2f

White solid, melting point: 89–91 °C. Yield (%): 26. I.R. cm⁻¹ (nujol): 1635, 3284. ¹H NMR (CDCl₃/TMS) ppm (δ): 0.80 (t, 3H, CH₃, hept., *J* = 6.10 Hz); 1.10 (d, 3H, CH₃, hept., *J* = 6.71 Hz); 1.10–2.10 (m, 15H, 7(CH₂), CH, hept. and pip.); 2.87 (d, 2H, CH₂, pip.); 3.49 (s, 2H, –CH₂–Ar); 3.93 (m, 1H, CH, hept., *J* = 6.71 and 7.93 Hz); 5.17 (d broad, 1H, (CO)NH disappearing on deuteration, *J* = 7.93 Hz); 7.15 (dd, 1H, H₅, arom., *J* = 8.54 Hz); 7.28 (d, 1H, H₄, arom.); 7.15 (d, 1H, H₂, arom., *J* = 8.54 Hz). MS: *m/z* 385 [MH⁺], 387 [MH⁺+2]. Anal. calcd. for C₂₀H₃₁Cl₂N₂O (MW 385.37): C, 62.33; H, 7.85; N, 7.27%; found: C, 62.10; H, 7.60; N, 7.00%.

6.2.17. 1-Benzyl-N-isopropylpiperidine-4-carboxamide 2g

Light-yellow solid, melting point: 143–145 °C. Yield (%): 35. I.R. cm⁻¹ (nujol): 1632, 3244. ¹H NMR (CDCl₃/TMS) ppm (δ): 1.15 (d, 6H, 2(CH₃), isopr., *J* = 6.59 Hz); 1.70–2.10 (m, 7H, 3(CH₂), CH, pip.); 2.90 (d, 2H, CH₂, pip.); 3.51 (s, 2H, –CH₂–Ph); 4.08 (m, 1H, CH, isopr., *J* = 6.59 Hz); 5.30 (s broad, 1H, (CO)NH disappearing on deuteration); 7.30–7.35 (m, 5H, arom.). MS: *m/z* 261 [MH⁺]. Anal. calcd. for C₁₆H₂₄N₂O (MW 260.37): C, 73.81; H, 9.29; N, 10.76%; found: C, 73.80; H, 9.10; N, 10.60%.

6.2.18. 1-(4-Chlorobenzyl)-N-isopropylpiperidine-4-carboxamide 2h

Light-yellow solid, melting point: 167–169 °C. Yield (%): 43. I.R. cm⁻¹ (nujol): 1629, 3249. ¹H NMR (CDCl₃/TMS) ppm (δ): 1.14 (d, 6H, 2(CH₃) isopr., *J* = 6.59 Hz); 1.60–2.10 (m, 7H, 3(CH₂), CH, pip.); 2.90 (d, 2H, CH₂, pip.); 3.46 (s, 2H, –CH₂–Ph); 4.09 (m, 1H, CH, isopr., *J* = 6.59 Hz); 5.30 (s broad, 1H, (CO)NH disappearing on deuteration); 7.28 (m, 4H, arom.). MS: *m/z* 295 [MH⁺], 297 [MH⁺+2]. Anal. calcd. for C₁₆H₂₃ClN₂O (MW 294.82): C, 65.18; H, 7.86; N, 9.50%; found: C, 64.90; H, 7.70; N, 9.50%.

6.2.19. 1-(2,4-Dichlorobenzyl)-N-isopropylpiperidine-4-carboxamide 2i

Light-yellow solid, melting point: 140–142 °C. Yield (%): 40. I.R. cm⁻¹ (nujol): 1638, 3286. ¹H NMR (CDCl₃/TMS) ppm (δ): 1.09 (d, 6H, 2(CH₃) isopr., *J* = 5.86 Hz); 1.50–2.10 (m, 7H, 3(CH₂), CH, pip.); 2.90 (d, 2H, CH₂, pip.); 3.50 (s, 2H, –CH₂–Ph); 4.10 (m, 1H, CH, isopr., *J* = 5.86 Hz); 5.20 (s broad, 1H, (CO)NH disappearing on deuteration); 7.20–7.40 (m, 3H, arom.). MS: *m/z* 329 [MH⁺], 331 [MH⁺+2]. Anal. calcd. for C₁₆H₂₂Cl₂N₂O (MW 329.26): C, 58.36; H, 6.73; N, 8.51%; found: C, 58.94; H, 6.70; N, 8.70%.

6.2.20. (1-Benzylpiperidin-4-yl) (3,4-dihydroquinolin-1(2H)-yl) methanone 2j

Oil Yield (%): 62. I.R. cm⁻¹ (nujol): 1660. ¹H NMR (CDCl₃/TMS) ppm (δ): 1.10–1.90 (m, 9H, H_{3,3'} dihydroq. and 3(CH₂), CH pip.); 2.63 (t, 2H, H_{4,4'} dihydroq., *J* = 6.71 Hz); 2.82 (d, 2H, CH₂, pip.); 3.39 (s, 2H, –CH₂–Ph); 3.70 (t, H_{2,2'} dihydroq., *J* = 6.71 Hz); 7.10–7.40 (m,

9H, arom.). MS: m/z 335 $[MH^+]$. Anal. calcd. for $C_{22}H_{26}N_2O$ (MW 334.45): C, 79.00%; H, 7.84%; N, 8.38%; found: C, 78.80%; H, 7.70%; N, 8.10%.

6.2.21. (1-(4-Chlorobenzyl)piperidin-4-yl) (3,4-dihydroquinolin-1(2H)-yl)methanone **2k**

Oil Yield (%): 91. I.R. cm^{-1} (nujol): 1631. 1H NMR ($CDCl_3/TMS$) ppm (δ): 1.10–1.90 (m, 9H, $H_{3,3'}$ dihydroq. and 3(CH_2), CH pip.); 2.60 (t, 2H, $H_{4,4'}$ dihydroq., $J = 6.71$ Hz); 2.80 (d, 2H, CH_2 , pip.); 3.40 (s, 2H, $-CH_2-Ar$); 3.67 (t, $H_{2,2'}$ dihydroq., $J = 6.71$ Hz.); 7.00–7.20 (m, 8H, arom.). MS: m/z 369 $[MH^+]$, 371 $[MH^++2]$. Anal. calcd. for $C_{22}H_{25}ClN_2O$ (MW 368.90): C, 71.63%; H, 6.83%; N, 7.59%; found: C, 71.70%; H, 6.90%; N, 7.70%.

6.2.22. (1-(2,4-Dichlorobenzyl)piperidin-4-yl) (3,4-dihydroquinolin-1(2H)-yl)methanone **2l**

Brown solid, melting point: 104–107 °C. Yield (%): 92. I.R. cm^{-1} (nujol): 1643. 1H NMR ($CDCl_3/TMS$) ppm (δ): 1.50–2.00 (m, 6H, $H_{3,3'}$ dihydroq. and 2(CH_2) pip.); 2.60 (t, 2H, $H_{3,3'}$ dihydroq., $J = 6.71$ Hz); 2.50–2.80 (m, 5H, $H_{4,4'}$ dihydroq. and 2(CH_2), CH pip.); 3.41 (s, 2H, $-CH_2-Ar$); 3.68 (t, $H_{2,2'}$ dihydroq., $J = 6.71$ Hz.); 7.00–7.40 (m, 7H, arom.). MS: m/z 403 $[MH^+]$, 405 $[MH^++2]$. Anal. calcd. for $C_{22}H_{24}Cl_2N_2O$ (MW 403.34): C, 65.51%; H, 6.00%; N, 6.95%; found: C, 65.50%; H, 6.10%; N, 6.90%.

6.2.23. (1-Benzylpiperidin-4-yl) (3,4-dihydroisoquinolin-2(1H)-yl)methanone **2m**

Brown solid, melting point: 82–85 °C. Yield (%): 43. I.R. cm^{-1} (nujol): 1631. 1H NMR ($CDCl_3/TMS$) ppm (δ): 1.50–2.00 (m, 6H, 3(CH_2) pip.); 2.46 (m, 1H, CH pip.); 2.80 (m, 4H, $H_{4,4'}$ dihydroq. and CH_2 pip.); 3.45 (s, 2H, $-CH_2-Ph$); 3.60–3.80 (dt, 2H, $H_{3,3'}$ dihydroq., $J = 5.49$ and 6.10 Hz.); 4.60 (d, 2H, $H_{1,1'}$ dihydroq., $J = 16.5$ Hz); 7.10–7.40 (m, 9H, arom.). MS: m/z 335 $[MH^+]$. Anal. calcd. for $C_{22}H_{26}N_2O$ (MW 334.45): C, 79.00%; H, 7.84%; N, 8.38%; found: C, 78.70%; H, 7.90%; N, 8.30%.

6.2.24. (1-(4-Chlorobenzyl)piperidin-4-yl) (3,4-dihydroisoquinolin-2(1H)-yl)methanone **2n**

Oil Yield (%): 64. I.R. cm^{-1} (nujol): 1624. 1H NMR ($CDCl_3/TMS$) ppm (δ): 1.50–2.00 (m, 6H, 3(CH_2) pip.); 2.45 (m, 1H, CH pip.); 2.80 (m, 4H, $H_{4,4'}$ dihydroq. and CH_2 pip.); 3.37 (s, 2H, $-CH_2-Ar$); 3.57–3.80 (dt, 2H, $H_{3,3'}$ dihydroq., $J = 5.49$ and 6.10 Hz.); 4.60 (d, 2H, $H_{1,1'}$ dihydroq., $J = 15.9$ Hz); 7.00–7.20 (m, 8H, arom.). MS: m/z 369 $[MH^+]$, 371 $[MH^++2]$. Anal. calcd. for $C_{22}H_{25}ClN_2O$ (MW 368.90): C, 71.63%; H, 6.83%; N, 7.59%; found: C, 71.50%; H, 6.80%; N, 7.30%.

6.2.25. (1-(2,4-Dichlorobenzyl)piperidin-4-yl) (3,4-dihydroisoquinolin-2(1H)-yl)methanone **2o**

Oil Yield (%): 95. I.R. cm^{-1} (nujol): 1640. 1H NMR ($CDCl_3/TMS$) ppm (δ): 1.54–2.16 (m, 6H, 3(CH_2) pip.); 2.50 (m, 1H, CH pip.); 2.80 (m, 4H, $H_{4,4'}$ dihydroq. and CH_2 pip.); 3.49 (s, 2H, $-CH_2-Ar$); 3.60–3.80 (dt, 2H, $H_{3,3'}$ dihydroq., $J = 5.49$ and 6.10 Hz.); 4.60 (d, 2H, $H_{1,1'}$ dihydroq., $J = 14.0$ Hz); 7.00–7.40 (m, 7H, arom.). MS: m/z 403 $[MH^+]$, 405 $[MH^++2]$. Anal. calcd. for $C_{22}H_{24}Cl_2N_2O$ (MW 403.34): C, 65.51%; H, 6.00%; N, 6.95%; found: C, 65.70%; H, 6.20%; N, 7.10%.

7. Pharmacology

7.1. Materials

The guinea pig brains and rat liver for the σ_1 and σ_2 receptor binding assays were commercially available (Harlan-Winkelmann, Borchon, Germany). The pig brains for the performance of the binding assay to the PCP-binding site of the NMDA receptor were a

kind donation of the local slaughterhouse (Coesfeld, Germany). Homogenizers: Elvehjem Potter (B. Braun Biotech International, Melsungen, Germany) and (Soniprep 150, MSE, London, UK). Centrifuges: Cooling centrifuge model Rotina 35R (Hettich, Tuttlingen, Germany) and High-speed cooling centrifuge model Sorvall RC-5C plus (Thermo Fisher Scientific, Langensfeld, Germany). Multiplates: standard 96-well multiplates (Diagonal, Muenster, Germany). Shaker: self-made device with adjustable temperature and tumbling speed (scientific workshop of the institute). Harvester: MicroBeta FilterMate-96 Harvester. Filter: Printed Filtermat Typ A and B. Scintillator: Meltilex (Typ A or B) solid state scintillator. Scintillation analyzer: MicroBeta Trilux (all Perkin Elmer LAS, Rodgau-Jügesheim, Germany).

7.2. Preparation of membrane homogenates from guinea pig brain

5 guinea pig brains were homogenized with the potter (500–800 rpm, 10 up-and-down strokes) in 6 volumes of cold 0.32 M sucrose. The suspension was centrifuged at $1200\times g$ for 10 min at 4 °C. The supernatant was separated and centrifuged at $23,500\times g$ for 20 min at 4 °C. The pellet was resuspended in 5–6 volumes of buffer (50 mM TRIS, pH 7.4) and centrifuged again at $23,500\times g$ (20 min, 4 °C). This procedure was repeated twice. The final pellet was resuspended in 5–6 volumes of buffer and stored at -80 °C in 1.5 mL portions containing about 1.5 mg protein/mL.

7.3. Preparation of membrane homogenates from rat liver

Two rat livers were cut into small pieces and homogenized with the potter (500–800 rpm, 10 up-and-down strokes) in 6 volumes of cold 0.32 M sucrose. The suspension was centrifuged at $1200\times g$ for 10 min at 4 °C. The supernatant was separated and centrifuged at $31,000\times g$ for 20 min at 4 °C. The pellet was resuspended in 5–6 volumes of buffer (50 mM TRIS, pH 8.0) and incubated at room temperature for 30 min. After the incubation, the suspension was centrifuged again at $31,000\times g$ for 20 min at 4 °C. The final pellet was resuspended in 5–6 volumes of buffer and stored at -80 °C in 1.5 mL portions containing about 2 mg protein/mL.

7.4. Preparation of membrane homogenates from pig brain cortex

Fresh pig brain cortex was homogenized with the potter (500–800 rpm, 10 up-and-down strokes) in 6 volumes of cold 0.32 M sucrose. The suspension was centrifuged at $1200\times g$ for 10 min at 4 °C. The supernatant was separated and centrifuged at $31,000\times g$ for 20 min at 4 °C. The pellet was resuspended in 5–6 volumes of TRIS/EDTA buffer (5 mM/1 mM, pH 7.5) and centrifuged again at $31,000\times g$ (20 min, 4 °C). The final pellet was resuspended in 5–6 volumes of buffer and stored at -80 °C in 1.5 mL portions containing about 0.8 mg protein/mL.

7.5. Protein determination

The protein concentration was determined by the method of Bradford [37], modified by Stoscheck [38]. The Bradford solution was prepared by dissolving 5 mg of Coomassie Brilliant Blue G 250 in 2.5 mL of EtOH (95%, v/v). 10 mL deionized H_2O and 5 mL phosphoric acid (85%, m/v) were added to this solution, the mixture was stirred and filled to a total volume of 50.0 mL with deionized water. The calibration was carried out using bovine serum albumin as a standard in 9 concentrations (0.1, 0.2, 0.4, 0.6, 0.8, 1.0, 1.5, 2.0 and 4.0 mg/mL). In a 96-well standard multiplate, 10 μ L of the calibration solution or 10 μ L of the membrane receptor preparation were mixed with 190 μ L of the Bradford solution, respectively. After 5 min, the UV absorption of the protein-dye complex at $\lambda = 595$ nm

was measured with a platereader (Tecan Genios, Tecan, Crailsheim, Germany).

7.6. General procedures for the binding assays

The test compound solutions were prepared by dissolving approximately 10 μmol (usually 2–4 mg) of test compound in DMSO so that a 10 mM stock solution was obtained. To obtain the required test solutions for the assay, the DMSO stock solution was diluted with the respective assay buffer. The filtermats were pre-soaked in 0.5% aqueous polyethylenimine solution for 2 h at room temperature before use. All binding experiments were carried out in duplicates in the 96-well multiplates. The concentrations given are the final concentration in the assay. Generally, the assays were performed by addition of 50 μL of the respective assay buffer, 50 μL test compound solution in various concentrations (10^{-5} , 10^{-6} , 10^{-7} , 10^{-8} , 10^{-9} and 10^{-10} mol/L), 50 μL of corresponding radioligand solution and 50 μL of the respective receptor preparation into each well of the multiplate (total volume 200 μL). The receptor preparation was always added last. During the incubation, the multiplates were shaken at a speed of 500–600 rpm at the specified temperature. Unless otherwise noted, the assays were terminated after 120 min by rapid filtration using the harvester. During the filtration each well was washed five times with 300 μL of water. Subsequently, the filtermats were dried at 95 °C. The solid scintillator was melted on the dried filtermats at a temperature of 95 °C for 5 min. After solidifying of the scintillator at room temperature, the trapped radioactivity in the filtermats was measured with the scintillation analyzer. Each position on the filtermat corresponding to one well of the multiplate was measured for 5 min with the [^3H]-counting protocol. The overall counting efficiency was 20%. The IC_{50} -values were calculated with the program GraphPad Prism[®] 3.0 (GraphPad Software, San Diego, CA, USA) by non-linear regression analysis. Subsequently, the IC_{50} values were transformed into K_i -values using the equation of Cheng and Prusoff [39]. The K_i -values are given as mean value \pm SEM from three independent experiments.

7.7. Performance of the binding assays

7.7.1. σ_1 receptor

The assay was performed with the radioligand [^3H]-(+)-Pentazocine (22.0 Ci/mmol; Perkin Elmer). The thawed membrane preparation of guinea pig brain cortex (about 100 μg of the protein) was incubated with various concentrations of test compounds, 2 nM [^3H]-(+)-Pentazocine, and TRIS buffer (50 mM, pH 7.4) at 37 °C. The non-specific binding was determined with 10 μM unlabeled (+)-Pentazocine. The K_d -value of (+)-Pentazocine is 2.9 nM [40].

7.7.2. σ_2 receptor

The assay was performed with the radioligand [^3H]DTG (specific activity 50 Ci/mmol; ARC, St. Louis, MO, USA). The thawed membrane preparations (rat liver preparation containing 100 μg protein) were incubated with various concentrations of the test compound, 3 nM [^3H]DTG and buffer containing (+)-pentazocine (500 nM (+)-pentazocine in 50 mM TRIS, pH 8.0) at room temperature. The non-specific binding was determined with 10 μM non-labeled DTG. The K_d value is 17.9 nM [41].

7.7.3. PCP binding site of the NMDA receptor

The assay was performed with the radioligand [^3H]-(+)-MK 801 (22.0 Ci/mmol; Perkin Elmer). The thawed membrane preparation of pig brain cortex (about 100 μg of the protein) was incubated with various concentrations of test compounds, 2 nM [^3H] (+) MK 801,

and TRIS/EDTA buffer (5 mM/1 mM, pH 7.5) at room temperature. The non-specific binding was determined with 10 μM unlabeled (+) MK 801. The K_d -value of (+)-MK-801 is 2.26 nM [42].

Acknowledgment

The financial support of FRA 2012 (Research Fund University of Trieste-Italy) is gratefully acknowledged.

References

- [1] W.R. Martin, C.E. Eades, J.A. Thompson, R.E. Huppler, *J. Pharmacol. Exp. Ther.* 197 (1976) 517–532.
- [2] A.L. Gundlach, B.L. Largent, S.H. Snyder, *Eur. J. Pharmacol.* 113 (1985) 465–466.
- [3] S.B. Hellewell, W.D. Bowen, *Brain Res.* 527 (1990) 235–236.
- [4] Y. Itzhak, I. Stein, *Brain Res.* 566 (1991) 166–172.
- [5] R. Quirion, W.D. Bowen, Y. Itzhak, J.L. Junien, J.M. Mustacchio, R.B. Rothman, T.P. Su, S.W. Tam, D.P. Taylor, *Trends Pharmacol. Sci.* 13 (1992) 85–86.
- [6] S.B. Hellewell, A. Bruce, G. Feinstein, J. Orringer, W. Williams, W.D. Bowen, *Eur. J. Pharmacol.* 268 (1994) 9–18.
- [7] M. Hanner, F. Moebius, A. Flandorfer, H.G. Knaus, J. Striessnig, E. Kemper, H. Glossmann, *Proc. Natl. Acad. Sci.* 93 (1996) 8072–8077.
- [8] R. Kekuda, P.D. Prasad, Y.J. Fei, F.H. Leibach, V. Ganapathy, *Biochem. Biophys. Res. Commun.* 229 (1996) 553–558.
- [9] P.D. Lupardus, R.A. Wilke, E. Aydar, C.P. Palmer, Y. Chen, A.E. Ruoho, M.B. Jackson, *J. Physiol.* 526 (2000) 527–539.
- [10] W. Hong, L.L. Werling, *Eur. J. Pharmacol.* 408 (2000) 117–125.
- [11] B.J. Vilner, W.D. Bowen, *J. Pharmacol. Exp.* 292 (2000) 900–911.
- [12] (a) T. Hayashy, T.P. Su, *Cell* 131 (2007) 596–610;
(b) S.I. Tsai, T. Hayashy, T. Mori, T.P. Su, *Cent. Nerv. Syst. Agents Med. Chem.* 9 (2009) 184–189;
(c) T. Mori, T. Hayashy, E. Hayashy, T.P. Su, *PLoS One* 8 (2013) e76941.
- [13] J. Xu, C. Zeng, W. Chu, F. Pan, J.M. Rothfuss, F. Zhang, Z. Tu, D. Zhou, D. Zeng, S. Vangveravong, F. Johnston, D. Spitzer, K.C. Chang, R.S. Hotchkiss, W.G. Hawkins, K.T. Wheeler, R.H. Mach, *Nat. Comm.* 2 (2011) 380.
- [14] K.W. Crawford, W.D. Bowen, *Cancer Res.* 62 (2002) 313–322.
- [15] K.W. Crawford, K.W. Coop, W.D. Bowen, *Eur. J. Pharmacol.* 443 (2002) 207–209.
- [16] T. Hayashy, T.P. Su, *Proc. Natl. Acad. Sci. U. S. A.* 98 (2001) 491–496.
- [17] Z. Wu, W.D. Bowen, *J. Biol. Chem.* 283 (2008) 28198–28215.
- [18] N.A. Colabufo, F. Berardi, M. Contino, M. Niso, C. Abate, R. Perrone, V. Tortorella, *Naunyn Schmiedeberg. Arch. Pharmacol.* 370 (2004) 106–113.
- [19] A. Azzariti, N.A. Colabufo, F. Berardi, L. Porcellini, M. Niso, G.M. Simone, R. Perrone, *A. Mol. Cancer Ther.* 5 (2006) 1807–1816.
- [20] B.R. de Costa, W.D. Bowen, S.B. Hellewell, J.M. Walker, A. Thurkauf, A.J. Jacobson, K.C. Rice, *FEB Lett.* 251 (1989) 53–58.
- [21] D. Fontanilla, M. Johannessen, A.R. Hajipour, N.V. Cozzi, M.B. Jackson, A.E. Ruoho, *Science* 323 (2009) 934–937.
- [22] (a) D. Zampieri, M.G. Mamolo, E. Laurini, C. Zanette, C. Florio, S. Collina, D. Rossi, O. Azzolina, L. Vio, *Eur. J. Med. Chem.* 44 (2009) 124–130;
(b) D. Zampieri, M.G. Mamolo, E. Laurini, C. Florio, C. Zanette, M. Fermeglia, P. Posocco, M. Paneni, S. Pricl, L. Vio, *J. Med. Chem.* 52 (2009) 5380–5393.
- [23] E. Laurini, V. Dal Col, M.G. Mamolo, D. Zampieri, P. Posocco, M. Fermeglia, L. Vio, S. Pricl, *ACS Med. Chem. Lett.* 2 (2011) 834–839.
- [24] E. Laurini, D. Marson, V. Dal Col, M. Fermeglia, M.G. Mamolo, D. Zampieri, L. Vio, S. Pricl, *Mol. Pharm.* 9 (2012) 3107–3126.
- [25] D. Zampieri, E. Laurini, L. Vio, S. Golob, M. Fermeglia, S. Pricl, M.G. Mamolo, *Bioorg. Med. Chem. Lett.* 24 (2014) 1021–1025.
- [26] (a) S. Collina, G. Loddio, M. Urbano, L. Linati, A. Callegari, F. Ortuso, S. Alcaro, C. Laggner, T. Langer, O. Prezzavento, G. Ronsisvalle, O. Azzolina, *Bioorg. Med. Chem.* 15 (2007) 771–783;
(b) D. Rossi, M. Urbano, A. Pedrali, M. Serra, D. Zampieri, M.G. Mamolo, C. Laggner, C. Zanette, C. Florio, D. Schepmann, B. Wünsch, O. Azzolina, S. Collina, *Bioorg. Med. Chem.* 18 (2010) 1204–1212;
(c) D. Rossi, A. Pedrali, M. Urbano, R. Gaggeri, M. Serra, L. Fernandez, M. Fernandez, J. Caballero, S. Ronsisvalle, O. Prezzavento, D. Schepmann, B. Wünsch, M. Peviani, D. Curti, O. Azzolina, S. Collina, *Bioorg. Med. Chem.* 19 (2011) 6210–6224;
(d) D. Rossi, A. Marra, P. Picconi, M. Serra, L. Catenacci, M. Sorrenti, E. Laurini, M. Fermeglia, S. Pricl, S. Brambilla, N. Almirante, M. Peviani, D. Curti, S. Collina, *Bioorg. Med. Chem.* 21 (2013) 2577–2586;
(e) D. Rossi, A. Pedrali, R. Gaggeri, A. Marra, L. Pignataro, E. Laurini, V. DalCol, M. Fermeglia, S. Pricl, D. Schepmann, B. Wünsch, M. Peviani, D. Curti, S. Collina, *Chem. Med. Chem.* 8 (2013) 1514–1527;

- (f) D. Rossi, A. Pedrali, A. Marra, L. Pignataro, D. Schepmann, B. Wünsch, L. Ye, K. Leuner, M. Peviani, D. Curti, O. Azzolina, S. Collina, *Chirality* 25 (2013) 814–822.
- [27] T. Schläger, D. Schepmann, K. Lehmkuhl, J. Holenz, J.M. Vela, H. Buschmann, B. Wünsch, *J. Med. Chem.* 54 (2011) 6704–6713.
- [28] (a) Y.H. Huang, P.S. Hammond, B.R. Whirrett, R.J. Kuhner, L. Wu, S.R. Childers, R.H. Mach, *J. Med. Chem.* 41 (1998) 2361–2370;
(b) Y.H. Huang, P.S. Hammond, L. Wu, R.H. Mach, *J. Med. Chem.* 44 (2001) 4404–4415.
- [29] C. Meyer, D. Schepmann, S. Yanagisawa, J. Yamaguchi, V. Dal Col, E. Laurini, K. Itami, S. Pricl, B. Wünsch, *J. Med. Chem.* 55 (2012) 8047–8065.
- [30] M.R. Lee, Y. Duan, P.A. Kollman, *Proteins* 39 (2000) 309–316.
- [31] G.M. Morris, R. Huey, W. Lindstrom, M.F. Sanner, R.K. Belew, D.S. Goodsell, A.J. Olson, *J. Comput. Chem.* 30 (2009) 2785–2791.
- [32] D.A. Case, T.A. Darden, T.E. Cheatham III, C.L. Simmerling, J. Wang, R.E. Duke, R. Luo, R.C. Walker, W. Zhang, K.M. Merz, B. Roberts, S. Hayik, A. Roitberg, G. Seabra, J. Swails, A.W. Goetz, I. Kolossváry, K.F. Wong, F. Paesani, J. Vanicek, R.M. Wolf, J. Liu, X. Wu, S.R. Brozell, T. Steinbrecher, H. Gohlke, Q. Cai, X. Ye, J. Wang, M.-J. Hsieh, G. Cui, D.R. Roe, D.H. Mathews, M.G. Seetin, R. Salomon-Ferrer, C. Sagui, V. Babin, T. Luchko, S. Gusarov, A. Kovalenko, P.A. Kollman, *AMBER 12*, University of California, San Francisco, 2012.
- [33] W.L. Jorgensen, J. Chandrasekhar, J.D. Madura, R.W. Impey, M.L. Klein, *J. Chem. Phys.* 79 (1983) 926–935.
- [34] For a list of recent, successful applications of the MM/PBSA methodology in related topics from our group see, for instance: a) E. Laurini, P. Posocco, M. Fermeglia, D.L. Gibbons, A. Quintás-Cardama, S. Pricl, *Mol. Oncol.* 7 (2013) 968–975;
b) X. Liu, C. Liu, E. Laurini, P. Posocco, S. Pricl, F. Qu, P. Rocchi, L. Peng, *Mol. Pharm.* 9 (2012) 470–481;
c) F. Bozzi, E. Conca, E. Laurini, P. Posocco, A. Lo Sardo, G. Jocollè, R. Sanfilippo, A. Gronchi, F. Perrone, E. Tamborini, G. Pelosi, M.A. Pierotti, R. Maestro, S. Pricl, S. Pilotti, *Lab. Investig.* 93 (2013) 1232–1240;
d) D.L. Gibbons, S. Pricl, H. Kantarjian, J. Cortes, A. Quintás-Cardama, *Cancer* 118 (2012) 293–299;
e) M.A. Pierotti, E. Tamborini, T. Negri, S. Pricl, S. Pilotti, *Nat. Rev. Clin. Oncol.* 8 (2011) 161–170;
f) P. Dileo, S. Pricl, E. Tamborini, T. Negri, S. Stacchiotti, A. Gronchi, P. Posocco, E. Laurini, P. Coco, E. Fumagalli, P.G. Casali, S. Pilotti, *Int. J. Cancer* 128 (2011) 983–990.
- [35] (a) A. Onufriev, D. Bashford, D.A. Case, *J. Phys. Chem. B* 104 (2000) 3712–3720;
(b) M. Feig, A. Onufriev, M.S. Lee, W. Im, D.A. Case, C.L. Brooks, *J. Comput. Chem.* 25 (2004) 265–284.
- [36] http://www.esteco.com/home/mode_frontier/mode_frontier.html.
- [37] M.M. Bradford, *Anal. Biochem.* 72 (1976) 248–254.
- [38] C. Stoscheck, *Methods Enzym.* 182 (1990) 50–68.
- [39] Y. Cheng, H.W. Prusoff, *Biochem. Pharmacol.* 22 (1973) 3099–3108.
- [40] D.L. De-Haven-Hudkins, L.C. Fleissner, F.Y. Ford-Rice, *Eur. J. Pharmacol. Mol. Pharmacol. Sect.* 227 (1992) 371–378.
- [41] R.H. Mach, C.R. Smith, S.R. Childers, *Life Sci.* 57 (1995) 57–62.
- [42] T. Utech (Ph.D. thesis), 2003, University of Fribourg, Germany.